



Evaluating Headway Control Using Range Versus Range-Rate Relationships

P. FANCHER & Z. BAREKET

To cite this article: P. FANCHER & Z. BAREKET (1994) Evaluating Headway Control Using Range Versus Range-Rate Relationships, Vehicle System Dynamics, 23:1, 575-596, DOI: [10.1080/00423119408969076](https://doi.org/10.1080/00423119408969076)

To link to this article: <http://dx.doi.org/10.1080/00423119408969076>



Published online: 27 Jul 2007.



Submit your article to this journal [↗](#)



Article views: 62



View related articles [↗](#)



Citing articles: 12 View citing articles [↗](#)

Evaluating Headway Control Using Range Versus Range-Rate Relationships

P. FANCHER* and Z. BAREKET*

SUMMARY

This paper uses range versus range-rate diagrams to illustrate concepts concerning the objectives of headway control, linear trajectories in the range versus range-rate space, and the influences of acceleration/deceleration limits on headway control systems. Relationships illustrated in range versus range-rate diagrams are used in evaluating first, second, and higher order systems for automatically controlling headway. Ideas for comparing driver control of headway with automatic control of headway are presented.

1. INTRODUCTION

Headway control pertains to the process of establishing and maintaining a desired range between a following vehicle and the vehicle preceding or leading it. This headway keeping function is performed manually by the drivers of current cars, buses, and trucks. However, many researchers within and outside of industry have been studying means for automatically controlling headway [e.g., 1, 2, 3]. These headway control systems are often called “intelligent cruise control (ICC)” systems in that they represent an extension of conventional cruise control (CCC) systems which are speed regulators. By adding equipment for measuring or determining the range to the vehicle ahead and by using that information to control both velocity and headway, research and development engineers and scientists have modified conventional vehicles to build working prototypes of vehicles equipped with intelligent cruise control [e.g., 2, 4, 5]. These prototype vehicles are useful for investigating the utility and acceptability of autonomous intelligent cruise control systems (AICC) [4, 6].

Currently, work aimed at evaluating and improving the performance of vehicles equipped with headway control systems for achieving ICC or AICC functionality is just beginning. Research investigators faced with evaluating the performance of an AICC system do not have a body of past experience to use in selecting an evaluation process. In the case of manual driving, there are

* The University of Michigan Transportation Research Institute, 2901 Baxter Road, Box 2150, Ann Arbor, Michigan 48109-2150, USA.

models of human performance that are used by highway engineers to study traffic flow [7, 8]. However, even the "microscopic" versions of these models do not seem to be useful for studying headway control – other than to indicate that drivers appear to be poor at maintaining a stable headway in dense traffic streams. Given a lack of applicable techniques, the purpose of this paper is to present basic concepts, derived from fundamental kinematical and dynamical relationships, which will aid researchers in designing headway control algorithms and in interpreting results obtained during the operation of prototype AICC vehicles.

The concepts addressed in this work are intended for application to cars, trucks, and buses but the ideas can be applied to trains, light rail vehicles, subways, people-movers, ships, etc. (i.e., all surface vehicles that travel along common paths). Clearly, an essential element of any system for controlling headway is a means for sensing the range between a following vehicle and its preceding vehicle. This paper emphasizes relationships between this range and its time rate of change ("range-rate").

Sensors have been developed to furnish both range and range rate information using microwave radar, infrared, or techniques based upon visible light. In cases where "time of flight" measurements are used to determine range, an approximate differentiator is used to determine range-rate. However, it seems possible that global or local positioning systems or track-based positioning systems might be used to determine range and range-rate in non-autonomous applications.

With regard to highway vehicles, the ideas presented here apply to various conditions of longitudinal control, including the AICC mode, manual driving, switching from conventional cruise control to manual control, and cases calling for driver intervention in the AICC mode.

2. DESCRIPTION OF THE HEADWAY CONTROL PROBLEM

The headway control problem may be stated as that of developing a system to maintain a desired headway by modulating the speed of the following vehicle. As illustrated in Figure 1, the headway range (R) and the range-rate (dR/dt) describe the relative position and relative velocity between the two vehicles. The objective of the headway control system is to use measured values of

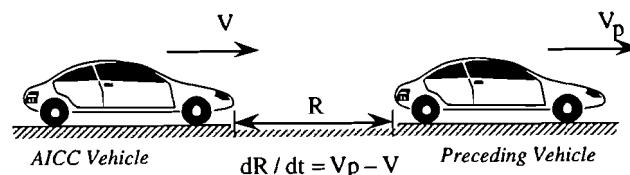


Fig. 1. Headway range (R) and range-rate (dR/dt).

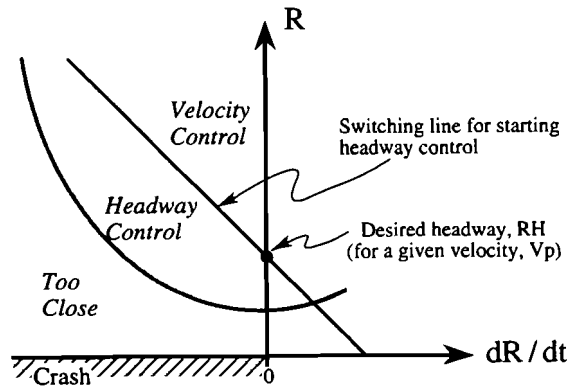


Fig. 2. Generic range versus range-rate diagram.

dR/dt and R to maintain a *specifically desired value* of headway range (R_H) corresponding to the condition $V = V_p$, where V is the velocity of the AICC vehicle and V_p is the velocity of the preceding vehicle.

Previous work has indicated that a range versus range-rate diagram (like Fig. 2) has benefits for displaying basic elements of the headway control problem [3, 9]. The desired headway range and velocity for headway-keeping at a given velocity is denoted by the point $(0, R_H)$ located on the vertical axis, corresponding to $dR/dt = 0$. As indicated in Figure 2, various regions of the $(dR/dt, R)$ space correspond to various control activities such as velocity control, headway control, and driver intervention as needed when the preceding vehicle is too close. Also, the boundaries between the regions shown in Figure 2, correspond to activities that are associated with transitions between operating situations. For example, Figure 2 shows a straight line passing through R_H that is labeled, "switching line for starting headway control."

The next two sections explain qualitative and quantitative properties of $(dR/dt, R)$ diagrams. These properties are useful for understanding reasons for setting the locations of boundaries between the various control activities. Ultimately, such diagrams will be used in a later section to illustrate the design features and evaluate the performance capabilities of an existing headway control system.

3. GENERIC PROPERTIES OF RANGE VERSUS RANGE-RATE DIAGRAMS

3.1 Qualitative Properties

The following properties apply to any two dimensional space defined by a variable and its derivative with respect to time. These same properties apply to phase plane diagrams for second order systems but more generally the relationships apply to systems of any order. In particular, even though conventional cruise control (CCC), ICC, and AICC systems may be of high order and

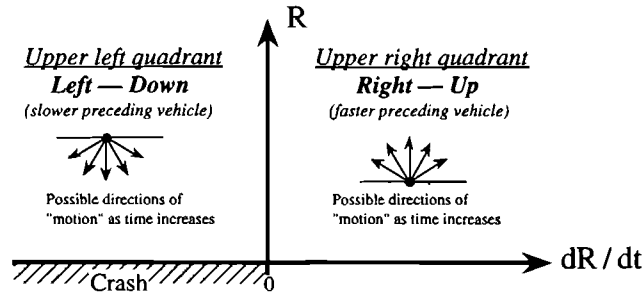


Fig. 3. Left-down and right-up directions of motion.

employ nonlinearities such as those associated with adaptive or sliding controls [10], the following qualitative results can still be used in evaluating the system's performance in attaining objectives concerning range and range-rate.

Figure 3 illustrates a basic principle concerning the direction of "motion" along any path in the $(dR/dt, R)$ space for $R > 0$. Since dR/dt is negative in the upper, left quadrant, R never increases along any trajectory in this quadrant. In physical terms this means that the following vehicle is closing in on the preceding vehicle because its velocity is greater than that of the preceding vehicle. Similar reasoning indicates that the vehicles are separating at any point for which dR/dt is positive; such that R must get larger in the upper, right quadrant of the $(dR/dt, R)$ space. Figure 3 illustrates this "left-down/right-up" principle. (This "principle" simply gives an air of formality to our basic understanding of what dR/dt means.)

Figure 4 presents qualitative examples illustrating the implications of the left-down/right-up principle applied to trajectories in the $(dR/dt, R)$ space. Straight line and parabolic trajectories will be examined in greater detail later. Nevertheless, these examples indicate reasons behind using R as the vertical axis and

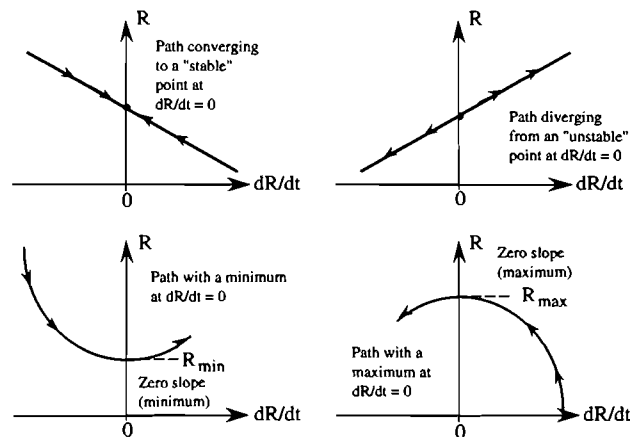


Fig. 4. Directions of motion on example paths.

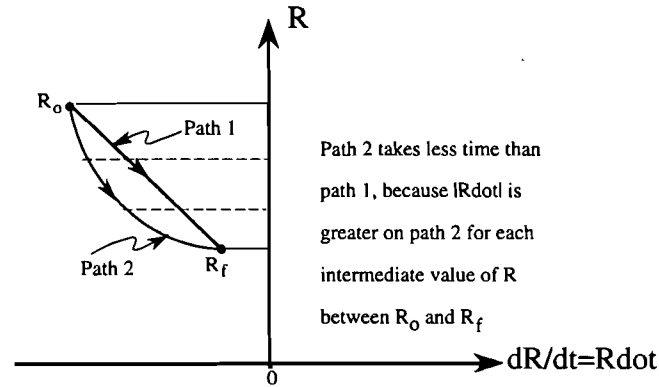


Fig. 5. Principle of shorter/longer time.

dR/dt as the horizontal axis. Specifically, the authors view the headway control problem as getting to a desired range using information about dR/dt to aid in getting there. For our purposes, maxima and minima and convergently stable and divergently unstable points along the vertical axis appear to us to be easier to describe and interpret.

The next qualitative idea has to do with the elapsed time required to go from one point to another along an allowable trajectory in the $(dR/dt, R)$ space. There is a principle of “shorter/longer time” involved here. The idea can readily be derived from the definition of dR/dt itself; viz.,

$$dR/dt = Rdot \quad (1)$$

where $Rdot$ represents the underlying expression for dR/dt in terms of R along a given trajectory.

Equation (1) can be separated into differentials and expressed in integral form as follows:

$$t_e = t - t_o = \int_{R_o}^{R_f} \frac{dR}{Rdot} \quad (2)$$

and where $t - t_o$ is the elapsed time (t_e) in traveling from R_o to R_f (in Figure 5) along the path defined by the expression for $Rdot$. In qualitative terms the integral in equation (2) implies that trajectories involving larger magnitudes of range-rate in going from one range to another will be traversed in less time than trajectories involving smaller magnitudes of $Rdot$ at the same values of R . Figure 5 illustrates by example the principle of shorter/longer time.

3.2 Quantitative Relationships for Specific Types of Headway Situations

Three types of relatively simple headway situations are particularly pertinent to the material presented later. These situations are representative of (a) closing on

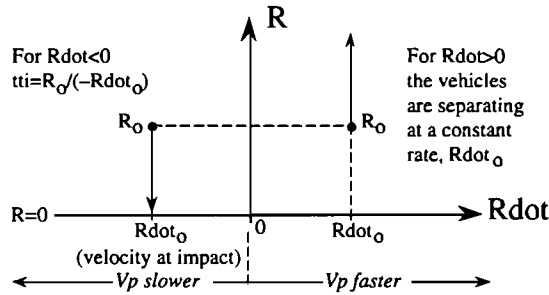


Fig. 6. Closing or separating at constant range-rate.

a preceding vehicle at constant range-rate, (b) tracking a preceding vehicle using a headway control system based upon a linear relationship between R and $R\dot{}$, and (c) operating at constant accelerations or decelerations by the following and preceding vehicles. The relationships between range (R) and range-rate ($R\dot{}$) are delineated in each of these situations and expressions for elapsed time along the trajectories involved are presented.

3.2.1 Situation (a). Closing or separating at constant range-rate

The applicable equations are as follows:

$$V = V_o, \text{ a constant} \quad (3)$$

$$V_p = V_{p_o}, \text{ another constant} \quad (4)$$

$$R\dot{=} = V_{p_o} - V_o = R\dot{=}_{o}, \text{ a constant value of } R\dot{=} \text{ here} \quad (5)$$

A generic illustration of this type of situation is presented in Figure 6. For $R\dot{=} < 0$, the time to impact (t_{ti}) is as follows for any value of R :

$$t_{ti} = \frac{R}{-R\dot{=}_{o}} \quad (6)$$

Clearly this is as simple a situation as anyone can imagine. However it happens frequently, since drivers tend to travel at fairly constant, but not identical, speeds. Interestingly, the time to impact (sometimes called the "time to collision") has been used in many human factors studies to describe the temporal separation between vehicles when drivers start braking [11]. Also, when t_{ti} is too small, the situation corresponds well to one in which conventional cruise control is no longer suitable and the driver needs to brake to prevent a collision.

3.2.2 Situation (b). A linear relationship between R and $R\dot{}$

This type of relationship has been employed in the control algorithm for a prototype headway control system [4]. The relationship is implemented by using the

conventional cruise control on the vehicle as part of the headway control system. If the frequency response of the cruise control is fast enough compared to that of the headway control system, the transfer function of the cruise control system will be approximately equal to one for the lower frequencies corresponding to AICC operation. This simply means that the headway control unit can be arranged to implement a linear relationship between R and \dot{R} using the notion that the velocity command (V_c) to the cruise control system will be roughly equal to the velocity of the AICC vehicle [9].

The applicable equation is as follows:

$$R = -T \cdot \dot{R} + RH \quad (7)$$

where T has units of time and $-T$ is the slope of this line in the (\dot{R}, R) space.

Equation 7 represents a linear first order differential equation. For RH equal to a constant, the solution corresponds to modulating deceleration so that R approaches RH exponentially; viz.,

$$R = R_0 \cdot e^{(-t_e/T)} + RH \cdot (1 - e^{(-t_e/T)}), \text{ for } RH = \text{a constant} \quad (8)$$

where R_0 is the initial value of R at $t_e = 0$. Note that T is the time constant of this first order system.

Clearly if RH is varying with time (such as if $RH(t_e) = TH \cdot V_p(t_e)$ where TH is called a "headway time" and $V_p(t_e)$ is the velocity of the preceding vehicle), the solution to equation (7) depends upon the forcing function $RH(t_e)$.

The solution given in equation (8) can also be derived by computing the elapsed time from R_0 to R by evaluating the integral of dR/\dot{R} from R_0 to R ; viz., using equation (7),

$$\frac{dR}{\dot{R}} = \frac{-T(dR)}{(R - RH)} \quad (9)$$

Equation (8) may be derived from the integral of equation (9). (See Appendix A.)

Since the solution to equation (7) is very familiar, the dynamicist knows that the length of time for R to reach RH is infinite but R will get to 63 percent of the way from R_0 to RH for $t_e = T$, 95 percent of the way to RH for $t_e = 3T$, and 99 percent of the way for $t_e = 5T$. Figure 7 presents a prototypic example of an (\dot{R}, R) diagram for the situation with a linear relationship.

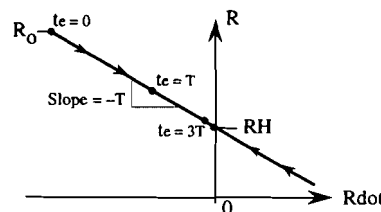


Fig. 7. Properties of a linear relationship between \dot{R} and R .

3.2.3 Situation (c). Constant decelerations

A typical set of parameters that represents this situation can be $V_{p0} =$ a constant, $Rdot < 0$, and $Vdot = -D$; where $Vdot$ is a deceleration level equal to D . The applicable equations are as follows:

$$V = V_o + A \cdot te \quad (10)$$

where A is the constant acceleration/deceleration of the AICC vehicle, and V_o is the initial value of V on the trajectory.

$$V_p = V_{p0} + A_p \cdot te \quad (11)$$

where A_p is the constant acceleration/deceleration of the preceding vehicle, and V_{p0} is the initial value of V_p on the trajectory.

From equations (10) and (11),

$$Rdot = Rdot_o + (A_p - A) \cdot te \quad (12)$$

where $Rdot_o$ is the initial (original) value of $Rdot$ on the trajectory.

From (12),

$$te = \frac{Rdot - Rdot_o}{A_p - A} \quad (13)$$

An interesting special case of equation (13) involves estimating the amount of time it would take to get from a point $(Rdot_o, R_o)$ to a point on the vertical axis defined by $Rdot = 0$ using a selected level of deceleration $D = (A_p - A)$. For example, if (a) V_p is a constant, (b) $Rdot_o < 0$, and (c) $-A = D$, the elapsed time to reach the $Rdot = 0$ is equal to $-Rdot_o/D$.

Equation (13) has a simple physical interpretation. At constant acceleration, the time to go from one speed to another is simply equal to the change in speed divided by the constant level of acceleration. This same result is derived in Appendix A using the integral of $dR/Rdot$. In any event, since $Rdot = 0$ is a special condition of importance to headway control, the time to reach $Rdot = 0$ is important; accordingly, for any $(Rdot, R)$ point in the region defined by $Rdot < 0$, the time to reach $Rdot = 0$ using a constant deceleration at level D is given by:

$$te(Rdot = 0) = \frac{-Rdot}{D}, \text{ for } Rdot < 0 \quad (14)$$

where $te(Rdot=0)$ is the time elapsed in reaching the vertical axis, i.e., $Rdot = 0$.

One can derive equations similar to equation (14) for all polarities of $Rdot$ and A , if one is interested.

Returning to equation (12), integrating with respect to time, and rearranging the result yields the following expression for constant deceleration paths in the (\dot{R} , R) space:

$$R - \frac{(\dot{R})^2}{2 \cdot (A_p - A)} = R_o - \frac{(\dot{R}_o)^2}{2 \cdot (A_p - A)} = R_{am} \quad (15)$$

where R_{am} is a constant for the trajectory. R_{am} is the value of R when $\dot{R} = 0$.

Equation (15) expresses an important idea. That is, given the “current” values (\dot{R}_c and R_c) of \dot{R} and R , one can compute the (\dot{R} , R) trajectory for any constant deceleration situation of interest. Rearranging equation (15) yields the following expression for all constant acceleration/deceleration trajectories:

$$R = R_{am} + \frac{(\dot{R})^2}{2 \cdot (A_p - A)} \quad (16)$$

Again returning to the special example when $\dot{R} < 0$, $A_p = 0$, and $-A = D$ (i.e., when the preceding vehicle is traveling at constant velocity and the AICC vehicle is decelerating from a speed greater than that of the preceding vehicle), the expression for the trajectory is:

$$R = R_{mn} + \frac{(\dot{R})^2}{2A} \quad (17)$$

where R_{mn} is the minimum of the trajectory which occurs when $\dot{R} = 0$.

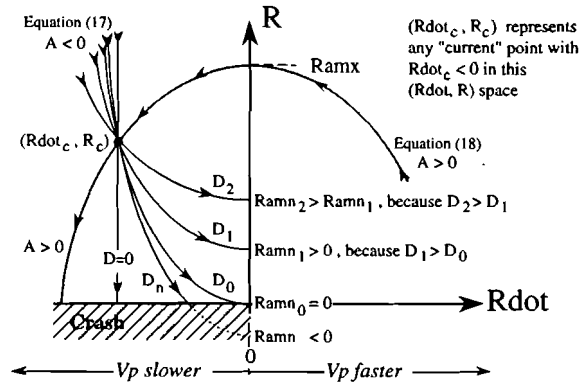
Correspondingly, for a situation in which $A_p = 0$ and $A > 0$ (which means forward acceleration of the AICC vehicle), the following expression applies:

$$R = R_{mx} - \frac{(\dot{R})^2}{2A} \quad (18)$$

where R_{mx} is the maximum of the trajectory which occurs when $\dot{R} = 0$.

The elapsed time to the maximum of the trajectory ($t_e(t_{max})$) of equation (15) from any original point (\dot{R}_o , R_o) such that $\dot{R}_o > 0$ is given by $t_e(t_{max}) = \dot{R}_o/A$; the time from the maximum for $\dot{R}_o < 0$ is given by $t_e(t_{max}) = -\dot{R}_o/A$.

In general the basic ideas here are that (a) the maximum or minimum of a constant acceleration or deceleration trajectory can be computed from any original (initial) point, and (b) the time between points on the trajectory can be easily computed using the simple expressions for the elapsed times to and from maxima or minima as the case may be. Figure 8 contains examples illustrating applications of these ideas. Appendix A contains equations which can



- Notes: (1) On the curves labeled “ $A > 0$ ”, “ $D = 0$ ”, and “ D_n ”, the magnitude of $Rdot$ at $R = 0$ is equal to the quantity “delta V” (ΔV) used in crash-worthiness studies.
- (2) The elapsed time to $Rdot = 0$ along the path labeled “ $D = 0$ ” is equal to $-R_c/Rdot_c$; the elapsed time to $Rdot = 0$ along the path labeled “ D_0 ” is equal to $-2R_c/Rdot_c$.
- (3) If $Ramn < 0$, the trajectory from $(Rdot_c, R_c)$ would lead to a crash (e.g. see the curve labeled “ D_n ”) even though the AICC vehicle is slowing down.

Fig. 8. Examples of parabolic trajectories for constant acceleration/deceleration situations.

be used to compute, for example, (a) the needed deceleration for insuring a minimum range or (b) combinations of range and range-rate at which a coast-down deceleration should start if the AICC vehicle is to avoid coming closer than desired to the preceding vehicle. For trajectories that could lead to impact, expressions for time to impact along a parabolic trajectory and relative velocity at impact are also given in the appendix.

4. EVALUATION OF THE DESIGN OF A HEADWAY CONTROL SYSTEM

The headway control system evaluated here has been described in reference [9]. The interactions between the basic components of the system are illustrated in Figure 9. The cruise-controlled vehicle is a complex dynamic system. The design of the needed velocity controller may be quite sophisticated with substantial non-linearities. The engine, drivetrain, etc. is a complicated dynamic system as is the braking system. When neither the brake nor the accelerator are actuated the vehicle coasts with a natural retardation due to tire rolling resistance, aerodynamic drag, drivetrain drag, and the grade of the roadway.

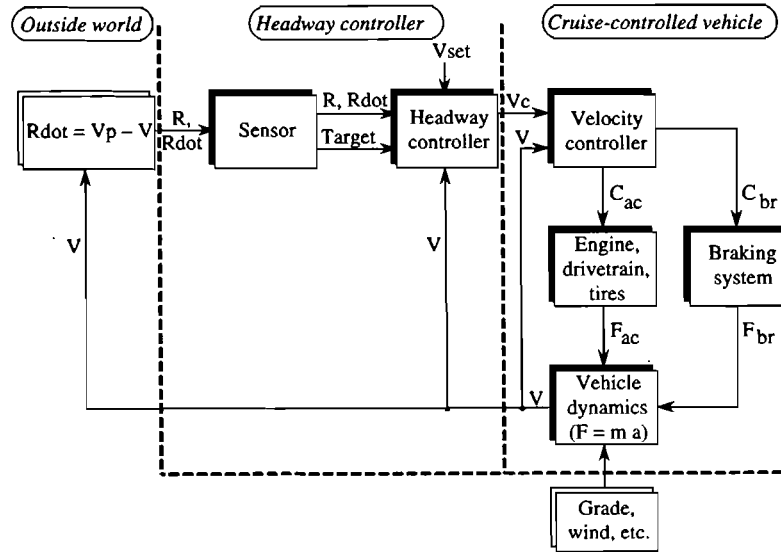


Fig. 9. Components of a headway control system for a cruise-controlled vehicle.

The velocity controller usually has a means for compensating for the effects of grade and rolling resistance on speed. Some form of integral control may be employed for this purpose.

There are many possible designs for cruise control systems. A relatively simple design based on proportional plus integral control with a switching arrangement to prevent integrator windup is described in [9]. As mentioned earlier, it is assumed that the vehicle has a well functioning velocity control system with a bandwidth that far exceeds that required for headway control. This means that V is approximately equal to V_c when the headway controller is determining V_c for headway control purposes. (To first approximation in the frequency range of the headway controller, $V/V_c \approx 1.0$.)

The headway controller is based upon the principles and relationships discussed earlier in this paper. In that regard it is convenient to describe the design of the headway controller using a range versus range-rate diagram. (See the design evaluation diagram, Figure 10.)

The design process consists of the following steps: (Design choices for an example set of parameters are included in this list of steps.)

1. Choose the desired headway distance for a selected velocity and headway time (Select point A).
 $RH = TH \cdot V_p$; where $TH = 1.5$ sec. and $V_p = 50$ mph (80 kph). (In this example TH is called the headway time and it is used to make RH a function of the velocity of the preceding vehicle. This means that closer ranges will be used at lower speeds.) Thus, we have that $RH = 110$ ft (33m).

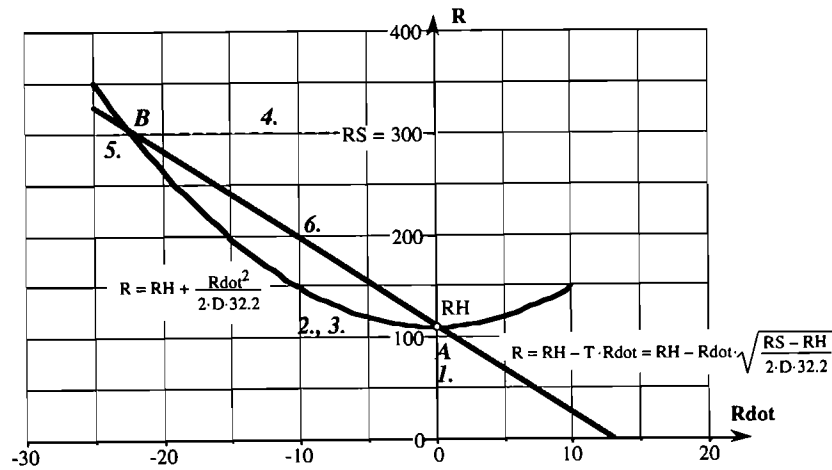


Fig. 10. Headway controller design process.

2. Choose the deceleration to be used.
 $D = \text{coasting (no braking)} = 0.04 \text{ g}$ for design purposes
3. Construct (plot) the parabola through $(0, R_H)$ using deceleration level D .
 (The parabola is $R = R_H + (R_{dot})^2 / (2D)$)
4. Choose the maximum range to consider. (This could be a reasonable range for the sensor or it might be chosen by selecting a maximum value of R_{dot} for design purposes or, hopefully the choice would satisfy both purposes.)
 e.g., let $R_s = 300 \text{ ft (90 m)}$ such that targets are well within the range of current sensors.
5. Determine point B from the intersection of $R = R_s$ and $R = R_H + (R_{dot})^2 / (2D)$.
6. Draw the line from point A to point B to determine its slope $(-T)$. Algebraically, $T = [(R_s - R_H) / (2D)]^{0.5} = [(300 - 110) / (0.08 \cdot 32.2)]^{0.5} = 8.6 \text{ sec}$ in this example.

The line with slope $-T$ is the switching line used in deciding when to apply headway control [9]. At ranges above this line the system operates as a conventional cruise control with the AICC vehicle travelling at the cruising speed set by the driver. Once the switching line is crossed, the system attempts to follow the switching line. However, immediately after crossing the switching line, the level of deceleration will not be large enough to force the system to follow the switching line dynamically. After crossing the switching line, the headway control applies the maximum deceleration available to the velocity control system. Let $R = R_0$ and $R_{dot} = R_{dot}_0$ indicate the point when and where the crossing occurs. After the crossing, the system is operating on the parabolic trajectory

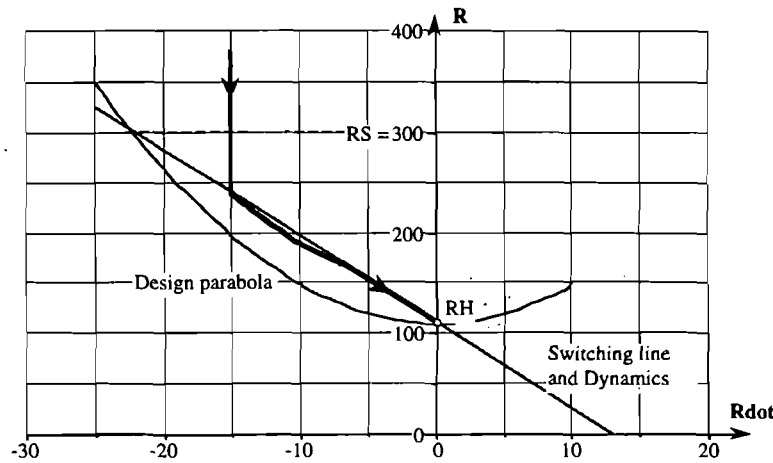


Fig. 11. Headway control trajectory when converging from $R\dot{o}_0 = 15$ ft/sec.

determined by the following equation:

$$R = R_{mn} + \frac{R\dot{o}^2}{2 \cdot D} \quad \text{where } R_{mn} = R_o - \frac{R\dot{o}_o^2}{2 \cdot D} \quad (19)$$

This parabola will lie between the switching line and the parabola labeled 2,3 in Figure 10. An example trajectory for $R\dot{o}_0 = 15$ ft/sec (10.2 mph, 16.3 kph) is shown in Figure 11.

This figure illustrates several qualities related to evaluating the performance of this design; viz.,

- The AICC vehicle starts to decelerate at a point which is neither too close nor too far away from the preceding vehicle for the level of deceleration available.
- The trajectory does not come closer to the preceding vehicle than the desired headway.
- The time to travel along the parabolic portion of the trajectory is less than it would have been travelling along the corresponding straight-line portion of the switching line.
- The system switches to a first order system before the desired range (RH) is reached.
- The point (0, RH) is a stable point that is approached exponentially.

Clearly, these qualities follow the principles and relationships presented earlier. The system follows the straight-line trajectory near RH because the acceleration control is being modulated to achieve the decreasing level of deceleration required to follow the straight-line trajectory designed into the headway controller. (That is, the accelerator is working against the natural retardation to produce the necessary deceleration.)

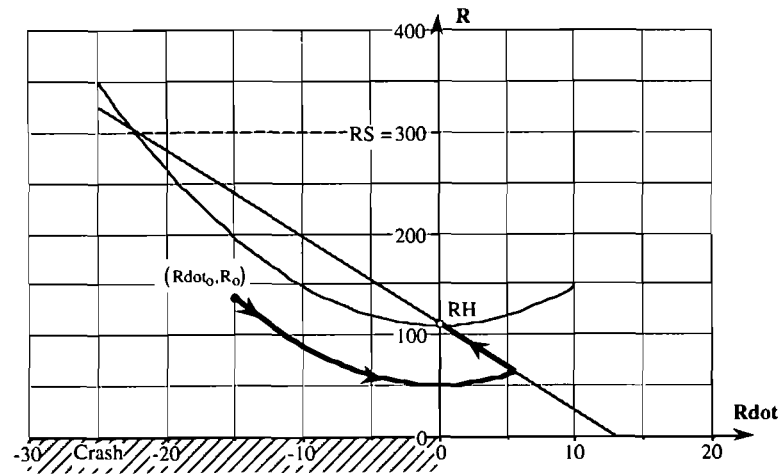


Fig. 12. Headway control trajectory when a target appears below the coastdown parabola.

The situation presented in Figure 11 pertains to closing in on and tracking a slower moving vehicle. In contrast, Figure 12 corresponds to a situation in which a target suddenly appears within a range value that is closer than that defined by the parabola for coastdown deceleration shown in Figure 10. This might happen on a curve, during a lane change, or through a cut-in by another vehicle. In this example the AICC vehicle would go closer to the preceding vehicle than desired, but the situation is not so bad that a collision or near miss would occur. As indicated in Figure 12, the AICC vehicle would slow to a speed that is less than that of the preceding vehicle and then gradually increase its speed along the straight-line towards the $(0, R_H)$ point.

If the headway is anticipated to be too short, the driver must intervene. A parabola can be defined based upon the maximum level of deceleration available under AICC control, to delineate the boundary of range and range-rate values below which a driver-alert warning might be given. In any case, of course, the driver must perform a supervisory function because the sensor may miss a target or there could be a stationary target in the road.

Figure 13 presents field data from a prototypic headway control system operating on the highway. Figure 13.a shows a typical result for closing on a slower moving vehicle. Figure 13.b shows a result when a target appeared at close range. These results indicate that the qualities described in this section can be realized in practice. The range versus range-rate diagram aids in evaluating system performance in terms of expected or desired operational characteristics of the system.

5. IDEAS CONCERNING DRIVER CONTROL OF HEADWAY

This section presents a driver-oriented view of the headway control functionality described in Section 4. The headway controller described previously will be

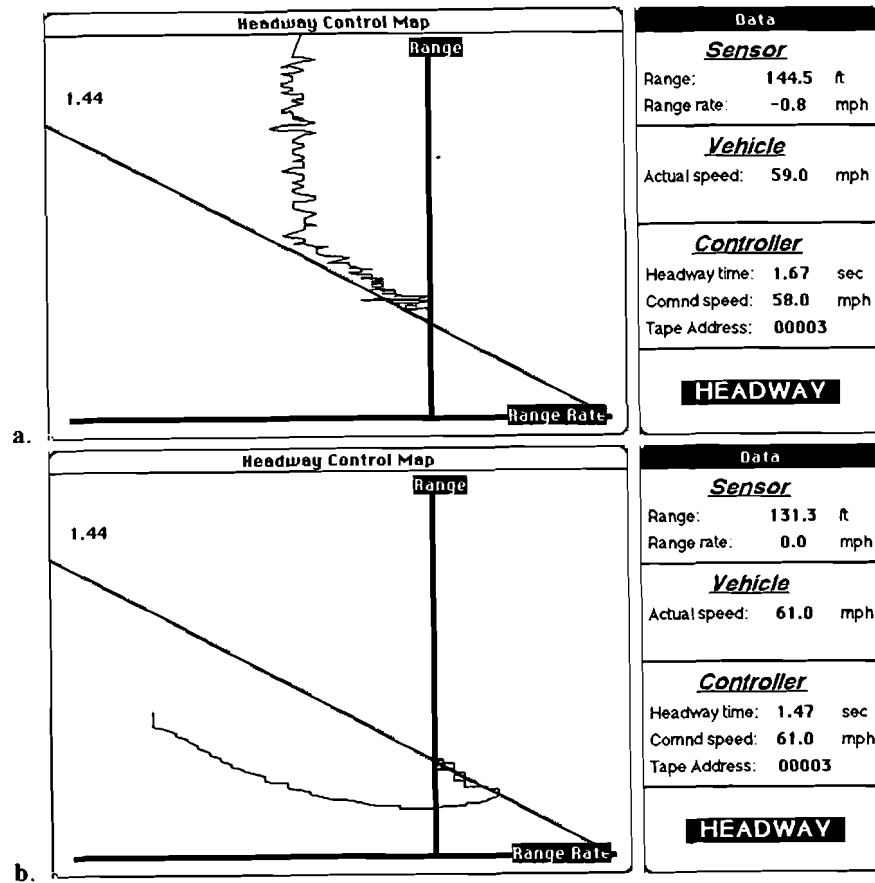


Fig. 13. Field data examples from a prototypic headway control system.

considered in the context of interpreting results obtained by measuring the time histories of range (R), range-rate ($Rdot$), and the velocity of the preceding vehicle (V_p) during normal driving without cruise or intelligent cruise control. It is presumed that it will be useful to process data from driver-controlled experiences in terms of headway time (TH), time constant (T), deceleration without braking (D), and deceleration with braking (Db).

This approach seems to be warranted because there does not appear to be a well developed science of driving. The authors have not been able to find results that address when and how drivers use coastdown deceleration to control vehicle speed and headway. And yet, our experience indicates that drivers on limited-access highways seldom brake, seldom even release the accelerator pedal fully, and indeed spend most of the time modulating the accelerator pedal to maintain speed and headway.

Given sensors for measuring R , $Rdot$, and V (and thereby V_p , since

$V_p = R_{dot} + V$), the problem is how to interpret and evaluate data obtained from driver controlled operation of the vehicle. The idea or hypothesis presented here, is to process the data in a manner which identifies driver-selected values for TH and T . The processed field data would be displayed in separate range versus range-rate diagrams for situations corresponding to braking, coasting, and accelerator modulation. If there is merit to this approach, an interpretive driver model of the form diagrammed in Figure 14 could be used to aid in evaluating driver/vehicle system performance.

The following philosophical reasoning is suggested as a basis for selecting a first approximation to use in iterating towards a theory of driver control of headway. As illustrated in Figure 14 the driver's sensory functions provide R , R_{dot} , and V data for use in selecting an objective headway range $RH(t+T)$ and also a predicted future position $R(t+T) \approx R(t) + T \cdot R_{dot}(t)$. It is postulated that the driver compares the predicted $R(t+T)$ with $RH(t+T)$ to decide on a velocity command (V_c) to make $R(t+T) = RH(t+T)$; viz.,

$$T \cdot (R_{dot}(t) + V - V_c) + R(t) = RH(t+T) \quad (20)$$

where $V - V_c$ is the change in velocity needed to make $R(t+T) = RH(t+T)$.

Solving equation (20) for V_c yields

$$V_c = R_{dot} + V + \frac{R}{T} - \frac{RH_p}{T} \quad (21)$$

where RH_p is the "previewed" headway range, i.e., the predicted value of RH at the time $t + T$ where T is called the "preview time" in driver modeling terminology.

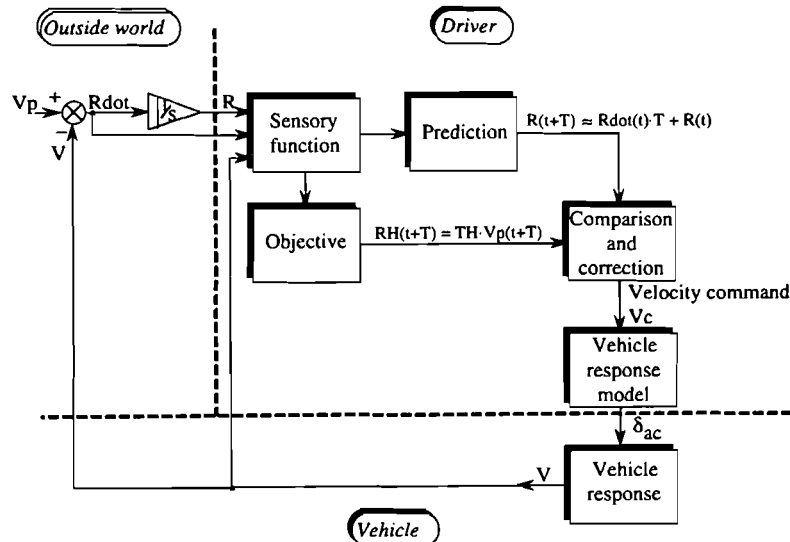


Fig. 14. A model for interpreting driver performance data.

ogy [12]. Incidentally, $\dot{R} + V = V_p$ the velocity of the preceding vehicle. Of course, V_c is similar to the velocity command used in the headway controller of Figure 10 since we set out to present a driver-oriented view of the headway control system described in Section 4.0. Nevertheless, equation (21) was derived using an entirely different approach based on philosophical reasoning concerning how people drive vehicles.

To complete the control loop in Figure 14, it is necessary to postulate that the driver knows where to set the accelerator pedal to obtain a desired velocity. The dynamic response of the vehicle to accelerator inputs is much quicker than that used by the driver in normal driving, so that the main time lag comes from the preview time (i.e., the time constant T).

Data collection and processing activities are planned to test this theory and to see if the data fits (correlates with) the postulated control system. It may be that nonlinear functions of parabolic or some other form will fit the data better than the linear expression presented in equation (21). In addition driver control of tracking may be expected to involve a pure time delay of some sort.

6. CONCLUSION

Concepts and ideas that can be portrayed in range versus range-rate diagrams have been applied to the headway control problem. These diagrams are useful in that they display the main elements of the problem, e.g. –

- the desired range when range-rate equals zero
- switching curves for transitioning from conventional cruise control to headway control
- a straight-line (linear) control algorithm of first order
- parabolic trajectories corresponding to constant deceleration or acceleration situations as may arise due to limits on the deceleration/acceleration available

Although the range versus range-rate diagram is two dimensional, it can be used in evaluating the performance of high order headway control systems. In a sense the range versus range-rate diagram can be thought of as a two dimensional slice through a system with many dimensions when the control system is of high order. For example, the control systems discussed in this paper are represented in detail by high order dynamic systems with substantial nonlinearities. Nevertheless, the range versus range-rate diagram presents the fundamental elements needed to determine and evaluate the quality of acquiring, closing, and following performance in the tracking of a preceding vehicle.

7. REFERENCES

1. Hedrick, K.: Longitudinal Control and Platooning: Collision Avoidance Systems for Intelligent Vehicles. SAE TOPTEC, Washington, D.C., April 13, 1993.

2. McCarter, O.T., Delco Electronics Corporation, and Schmidt, E.H. General Motors Corporation: Application of a 60 GHz Radar Sensor to Adaptive Cruise Control. Proceedings of the 26th International Symposium on Automotive Technology and Automation, Aachen, Germany, September 1993.
3. Bareket, Z., Fancher, P.S., and Johnson G.E.: Investigation of the Performance of a Headway-Control System for Commercial Vehicles. University of Michigan IVHS Technical Report #93-01, 1993.
4. Fancher, P.S., Ervin, R.D., Bareket, Z., and Johnson, G.E., University of Michigan Transportation Research Institute, Trefalt, M.J., Tiedecke, J., and Hagleitner, W., Leica AG, Switzerland: Intelligent Cruise Control: Performance Studies Based Upon an Operating Prototype. To be presented at the IVHS America Annual Meeting, April 17-20, 1994, Atlanta, GA.
5. Kishi, M., Watanabe, T., Hayafune, K., Yamada, K., and Hayakawa, H.: A Study on Safety Distance Control. Proceedings of the 26th International Symposium on Automotive Technology and Automation, Aachen, Germany, September 1993.
6. Becker, S., and Sonntag, J.: PROMETHEUS CED 5: Autonomous Intelligent Cruise Control Pilot Study Conducted by the Daimler Benz and Opel Demonstrators. TÜ Rheinland Institute of Traffic Safety, Central Department for Safety Research and Development Service, Cologne, Germany, November 1993.
7. Papageorgiou, M., and Ioannou, P.: Traffic Flow Modeling and Control and Intelligent Highway Systems (IVHS). Short Course notes, SSC Systems, June 1993.
8. May, A.D.: Traffic Flow Fundamentals. Prentice Hall, Englewood Cliffs, N.J., 1990.
9. Fancher, P.S., Bareket, Z., and Johnson, G.: Predictive Analysis of the Performance of a Headway Control System for Heavy Commercial Vehicles. Presented at the 13th IAVSD Symposium on the Dynamics of Vehicles on Road and Tracks, August 1993, Chengdu, China.
10. Slotine, J.-J.E., and Li, W.: Applied Nonlinear Control. Prentice Hall, Englewood Cliffs, New Jersey, 1991.
11. van der Horst, A.R.A.: A Time Based Analysis of Road User Behaviour in Normal and Critical Encounters. TNO Institute for Perception, Soesterberg, the Netherlands, 1990.
12. Guo, K., and Guan, H.: Modelling of Driver/Vehicle Directional Control System. Vehicle System Dynamics, Volume 22, Number 3-4, May/July 1993, pp.141-184, Swets & Zeitlinger.
13. NHTSA IVHS Plan. National Highway Traffic Safety Administration, U.S. Department of Transportation, Washington, D.C., June 12, 1992.

APPENDIX A

1. DERIVATION OF ELAPSED TIME (t_e)

1.1 With a Linear Relationship Between R and R_{dot}

The pertinent equation of the trajectory when R and R_{dot} are linearly related, is $R = -T dR/dt + R_H = -TR_{dot} + R_H$ (i.e., equation (7)). Assume R_H is a constant. Then,

$$t_e = \int_{R_o}^R \frac{dR}{(dR/dt)} = -T \cdot \int_{R_o}^R \frac{dR}{R - R_H} = -T \cdot \ln \left[\frac{R - R_H}{R_o - R_H} \right] \quad (A1)$$

where R_o is the original (initial) value of range on the trajectory and R_H is the final value of range for $t_e = \infty$.

Equation (A1) can be rewritten in terms of the exponential function; viz.,

$$\exp \left(\frac{-t_e}{T} \right) = \frac{R - R_H}{R_o - R_H} \quad (A2)$$

Equation (8) in the main text follows from equation (A2).

1.2 With Constant Deceleration of the Following Vehicle

The pertinent set of conditions in this case is $V_{p_o} = \text{const.}$, $R\dot{} < 0$, and $V\dot{} = -D$ where D is a constant level of deceleration of the following vehicle. The applicable equation of the trajectory is $R = R_{mn} + (R\dot{})^2/(2D)$ (i.e., equation (17)). Then,

$$t_e = \int_{R_o}^R \frac{dR}{(dR/dt)} = \int_{R_o}^R \frac{dR}{\sqrt{2D(R - R_{mn})}} \quad (A3)$$

$$t_e = \frac{[\sqrt{2D(R - R_{mn})} - \sqrt{2D(R_o - R_{mn})}]}{D} \quad (A4)$$

where R_{mn} is the minimum range of the trajectory which occurs when $R\dot{} = 0$. Using equation (17) to substitute appropriately in equation (A4), yields (for $R\dot{} < 0$ and $R\dot{}_o < 0$)

$$t_e = \left(\frac{R\dot{}_o}{D} - \frac{R\dot{}_o}{D} \right) \quad (A5)$$

where $(R\dot{}_o, R_o)$ is the original (initial) point and $(R\dot{}, R)$ is another point closer to $(0, R_{mn})$ than $(R\dot{}_o, R_o)$, that is, $R_o > R > R_{mn}$. It follows from (A5) that the time from $R\dot{}_o$ to the intercept of which $R\dot{} = 0$ is as follows:

$$t_e(R\dot{} = 0) = \frac{-R\dot{}_o}{D} \quad (A6)$$

Equation (A6) is restated using $R\dot{}_o$ instead of $R\dot{}_o$ in equation (14) because $R\dot{}_o$ could correspond to any arbitrary point on the trajectory when $R\dot{} < 0$.

2. INTERESTING EQUATIONS FOR CONSTANT ACCELERATION / DECELERATION TRAJECTORIES FOR $A_p = 0$

2.1 Computations Involving Decelerations for $R\dot{}_o < 0$

Each trajectory has a minimum at $R\dot{} = 0$. Equation (A7) defines this minimum in terms of an original point $(R\dot{}_o, R_o)$.

$$R_{mn} = R_o - \frac{(R\dot{}_o)^2}{2D} \quad (A7)$$

And equation (A8) defines the path of the trajectory for any point on the path.

$$R = R_{mn} + \frac{(R\dot{})^2}{2D} \quad (A8)$$

To get from (R_{dot_o}, R_o) to $(0, RH)$, the needed deceleration DH is as follows:

$$DH = \frac{R_o - RH}{2(R_{dot_o})^2} \quad (A9)$$

where RH is the desired value of R_{amn} .

If, for some point (R_{dot_o}, R_o) , $R_{amn} < 0$ for some choice of D (say D_n), there will be a crash on this trajectory when $R = 0$. From equations (A7) and (A8) the velocity at impact (V_i) is given by

$$V_i = -R_{dot_i} = \sqrt{-R_{amn}(2 \cdot D_n)} \quad (A10)$$

using equations (A5) and (A10), the time to impact (t_{ti}) is given by

$$t_{ti} = \frac{R_{dot_i}}{D_n} - \frac{R_{dot_o}}{D_n}, \text{ for } R_{dot_i} < 0 \text{ and } R_{dot_o} < 0 \quad (A11)$$

2.2 Computations Involving Accelerations ($A > 0$) for $R_{dot_o} < 0$

Each trajectory has a maximum at $R_{dot} = 0$. Equation (A12) defines this maximum.

$$R_{mx} = R_o + \frac{(R_{dot_o})^2}{2A} \quad (A12)$$

or,

$$R = R_{mx} - \frac{(R_{dot})^2}{2A} \quad (A13)$$

If the maximum value of this path is given by $R_{mx} = RM$, and the path goes through the point (R_{dot_o}, R_o) , then the deceleration involved with this path is

$$AM = \frac{RM - R_o}{2 \cdot (R_{dot_o})^2} \quad (A14)$$

If AM continues long enough, there will be a collision with a velocity of impact V_i which is given by

$$V_i = -R_{dot_i} = \sqrt{2 \cdot AM \cdot RM} \quad (A15)$$

The time to impact (t_{ti}) for $R_{dot_o} < 0$ is given by

$$t_{ti} = \frac{-R_{dot_i}}{AM} + \frac{R_{dot_o}}{AM} \quad (A16)$$

3. TIME AND DECELERATION INTENSITY FOR COLLISION AVOIDANCE

In conjunction with collision avoidance considerations, the intensity of counteraction taken (or what should be taken) by the driver is of major importance. In the context of this work, the intensity of counteraction is viewed as the level of deceleration (D) initiated and maintained by the following vehicle.

Under conditions of no-deceleration ($D = 0$), the time to impact (t_{ti_0}) is given by

$$t_{ti_0} = \frac{-R}{R\dot{o}_0}, \text{ for } R\dot{o}_0 < 0 \quad (A17)$$

The deceleration needed to go from any arbitrary point ($R\dot{o}_0, R_0$) for which $R\dot{o}_0 < 0$, to $(0, 0)$ is given by

$$DR = \frac{R\dot{o}_0^2}{2 \cdot R} = \frac{-R\dot{o}_0}{2 \cdot t_{ti_0}} \quad (A18)$$

Using this deceleration, the time to impact (t_{ti_D}) along the trajectory passing through $(0, 0)$ is

$$t_{ti_D} = \frac{-R\dot{o}}{DR} = 2 \cdot t_{ti_0} \quad (A19)$$

Equations (A17) and (A18) can be combined graphically to provide a crash avoidance diagram (see Figure A.1). This diagram pertains to a particular value of initial range rate ($R\dot{o}_0$). The linear plot (1), depicts the time to impact

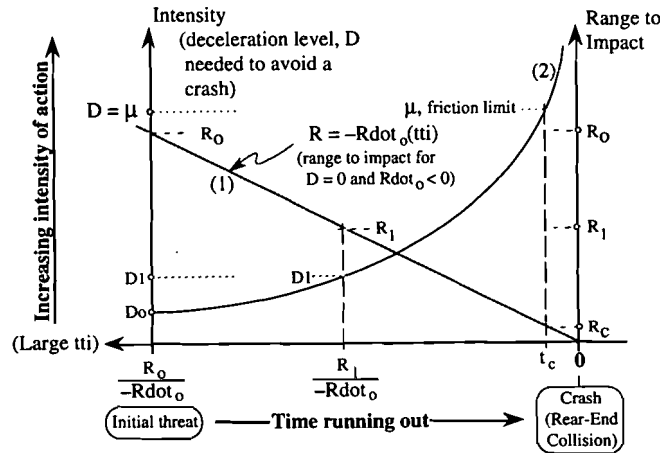


Fig. A.1. Intensity of action as time to crash runs out.

at each instantaneous range (given \dot{R}_0 , and with no deceleration). To avoid crash at any given range (e.g., R_1), the corresponding value of deceleration on plot (2) is required (e.g., D_1). At ranges below R_c , which corresponds to a required deceleration level equal to the friction limit (μ), a crash is imminent since the required deceleration capability is no longer available. Figure A.1 is similar to intensity versus time diagrams used in describing crash avoidance countermeasures for intelligent vehicle-highway systems (IVHS) [13].